Sensors and Materials, Vol. 36, No. 8 (2024) 3367–3380
MYU Tokyo

S & M 3737

Water-splitting Reactor Comprising a Combination of TiO_2-based Photoelectrochemical Cell and Serially Connected TiO_2/Se Heterojunction Photovoltaic Devices

Kenichi Takatsuki,[1] Riku Takahashi,[1] and Taizo Kobayashi[2*]

[1]Graduate School of Science and Engineering, Ritsumeikan University,
1-1-1 Noji Higashi, Kusatsu, Shiga 525-8577, Japan
[2]College of Science and Engineering, Ritsumeikan University,
1-1-1 Noji Higashi, Kusatsu, Shiga 525-8577, Japan

(Received April 15, 2024; accepted June 11, 2024)

Keywords: TiO_2, Sephotovoltaic cell, hydrogen production, bias voltage, on-chip device

In this paper, we report on a photocatalytic water-splitting device comprising a TiO_2 photoanode combined with Se/TiO_2 heterojunction photovoltaic (PV) devices. A Se/TiO_2 PV device can supply its photo-induced open circuit voltage to a TiO_2-Pt photoelectrochemical cell (PEC) in order to assist photoelectrolysis for H_2 and O_2 gas generation without external electrical sources. The open circuit voltage was increased from 0.65 V to approximately 3.2 V by the serial connection of five Se/TiO_2 PV devices. Hydrogen and oxygen bubbles were successfully generated by only light illumination without using any wired external voltage source. A photoanode with sol–gel derived porous TiO_2 films was used to increase the surface area to attain a stronger photocatalytic reaction. Microdot patterns of Pt were formed as the co-catalyst on a TiO_2 photoanode to suppress the back reaction of the photogenerated carrier. A Pt anode was formed on a glass substrate. Parameters related to the photocatalytic reaction, such as atmospheric pressure, the type of chemical additive, and the area ratio of Pt co-catalyst patterns to the surface area of the TiO_2 photoanode, were varied to generate a larger gas volume with the water-splitting device.

1. Introduction

Green hydrogen, which is harvested using only renewable energy without the need for fossil fuels and with little carbon emissions, has been attracting considerable attention as a storable clean fuel. Various large-scale industrial processes have been developed for hydrogen generation. However, most of those conventional methods were fossil-derived processes such as the Haber–Bosch process or a combination of natural-gas- and fossil-derived processes. Current industries desiring hydrogen generation technology include petroleum refining, ammonia production, vegetable oils, metal extraction, methanol, steel, and synthetic fuel.[1,2] Many researchers have developed solar-power-driven water-splitting devices as a carbon-neutral hydrogen generation technology. As such technologies, both electrochemical cells combined with solar cells and/or

*Corresponding author: e-mail: tkt07004@fc.ritsumei.ac.jp
https://doi.org/10.18494/SAM5075

ISSN 0914-4935
https://myukk.org/

photocatalytic water-splitting devices have been developed.[3–5] Powder-based and thin-film-based photocatalysts have been reported. For example, the use of the dual photocatalyst, which is made by combining different photocatalysts for hydrogen and oxygen generation, is one of the promising technical approaches of the powder-based photocatalyst for highly efficient water splitting.[6] Although the hydrogen generation cost is reduced to approximately 1.6 $/kg when the powder-based photocatalyst is used, the cost reduction of hydrogen generation is still an important issue.[2] Thin-film photocatalysts have advantages such as the availability of established manufacturing processes for on-chip implementation.[7] Eliminating the need for an electrical power supply from the photocatalytic water-splitting system is also important to achieve low-cost hydrogen generation. The miniaturization of water-splitting systems into on-chip devices will provide great opportunities for a safer on-site hydrogen harvesting technology using various types of accessible environmental energy. As a tandem configuration of a PV device and a photocatalyst, mesoporous metal oxide photocatalysts (e.g., SnO_2 and TiO_2) integrated on a Si photoanode have been reported.[8] Khaselev and Turner also reported a monolithic-structure water-splitting device with p/n-GaAs and p-$GaInP_2$.[9]

Our group previously proposed an optically driven gas generator on a chip with a thin-film photoelectrochemical cell (PEC) integrated with a thin-film heterojunction PV cell.[10] A Se/TiO_2 PV device can supply its light-induced open circuit voltage (V_{oc}) at 0.65 V as a DC bias voltage to a TiO_2-Pt PEC to accelerate photoelectrolysis for gas generation without the need for external electrical sources. The serial connection of thin-film PV devices makes it possible to increase the bias voltage with a simple device structure. The integration of thin-film-based PEC and PV devices on a chip also enables a compact gas generation system. Since TiO_2/ITO layers can be used as common materials for both TiO_2-Pt PEC and Se/TiO_2 PV devices, the proposed gas generator is applicable to on-chip integration. The ambient pressure, bias voltage, and filling area ratio of the Pt co-catalyst in the TiO_2 working electrode were varied during the characterization of water-splitting devices with constant UV illumination to increase the hydrogen generation rate.

2. Materials and Methods

2.1 Device design

We propose a water-splitting device composed of TiO_2-based PEC and Se thin-film PV devices, as illustrated in Fig. 1(a). An open circuit voltage of approximately 3.2 V can be supplied to the TiO_2 photocatalyst from five serially connected PV cells to support the photocatalytic water-splitting reaction. Figure 1(b) shows a schematic of the device structure of a single cell of a Se thin-film PV device. Sol-gel-derived mesoporous TiO_2 thin films (500 nm) with a large surface area were employed for the electrode to increase the hydrogen generation rate of PEC. It is widely known that anatase TiO_2 thin films generally exhibit a stronger photocatalytic activity than rutile TiO_2 thin films. In addition, it has been reported that sol–gel-derived porous TiO_2 thin films exhibit a much stronger photocatalytic performance than sputter-deposited TiO_2 thin films.[11] Moreover, it has also been reported that TiO_2 with an anatase/rutile mixture structure often exhibits a higher photocatalytic activity than that with a pure anatase or pure rutile

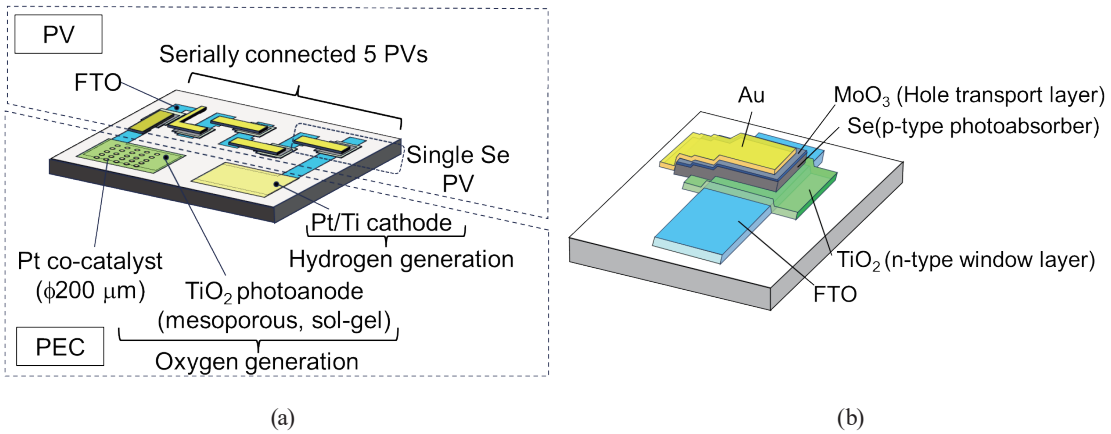

(a) (b)

Fig. 1. (Color online) (a) Device structure of the proposed water-splitting device composed of TiO_2-based PEC and serially connected Se thin-film PV devices. (b) Device structure of single cell of TiO_2/Se PV device.

structure.[12] For example, commercially available Degussa P25® (Sigma-Aldrich Co. LLC, USA) is widely known to have highly photoresponsive TiO_2 particles with anatase/rutile mixture crystallographic structures.[13] We previously investigated the photocatalytic activities of sputter-deposited and sol–gel-derived TiO_2 thin films with different anatase/rutile ratios and surface roughnesses.[14–17] Sol–gel-derived TiO_2 thin films exhibited the strongest photocatalytic activity among samples in our previous work.[14–17] Such photoanodes showed an anatase/rutile mixture and a mesoporous structure. Accordingly, TiO_2 films with anatase/rutile mixture crystallographic structures deposited by the sol–gel method were employed in this work. The porosity of TiO_2 can be changed by adjusting the amount of polyethylene glycol (PEG) added to the sol–gel precursor solution.[12] Circular Pt dot patterns of 0.2 mm diameter were formed on a TiO_2 photoanode as the co-catalyst to promote the water-splitting reaction. The electrical potential gradient at the Pt/TiO_2 interface promotes the transfer of photogenerated carriers from TiO_2 to Pt, resulting in the suppression of the hole-electron recombination, and the photocatalytic reaction can be enhanced.[18,19] A sputter-deposited Pt cathode (200 nm) was used as the electrode for hydrogen generation. The TiO_2 photoanode was illuminated by UV light through an indium-tin-oxide (ITO) transparent electrode layer from the substrate side. The exposed area of the TiO_2 photoanode was designed to be 66.5 mm^2. A Se thin-film PV device was developed as a superstrate structured device that can be illuminated from the substrate side. The PV device was composed of a p-type polycrystalline Se photoabsorber layer and an n-type TiO_2 window layer. Se is known as a promising photoabsorber material for visible light because of its very high absorption coefficient and bandgap energy of approximately 1.9 eV. In indoor PV applications under LED or cold fluorescent light illumination, the theoretical maximum limit of the conversion efficiency of the Se PV device is expected to be very high (approximately 55%).[20] MoO_3 (20 nm) was employed as a hole transport layer between Se and Au layers. The active area of a single TiO_2/Se PV device was designed to be 4 mm^2. Electrical lead patterns were insulated by nonconductive epoxy resin. A water-splitting reactor comprising TiO_2-based PEC and Se-based PV devices on a chip is characterized by varying the pressure, pH, and supplied bias voltage, as described in the experimental section.

2.2 Device fabrication

On-chip photocatalytic reactor devices were fabricated by the following steps (illustrated in Fig. 2):

1. FTO patterning: First, a fluorine-doped tin oxide (FTO) transparent conducting layer was patterned by HCl etching with a Mg particle catalyst. Photoresist mask patterns were formed on an FTO-coated glass substrate (Furuuchi Chemical Corporation, Japan). The photoresist (OFPR-800LB, 50CP) was prebaked at 115 ºC for 3 min after spin-coating at 300 rpm for 30 s. After UV exposure, the photoresist was postbaked at 180 ºC for 2 min. Patterns were formed by dipping samples in a developer solution. The area of FTO exposed to UV illumination was etched by applying 2.0 g of zinc powder (90%, Fujifilm Wako Pure Chemical, Japan) uniformly on the substrate and applying 2.5 mL of HCl (35%, Fujifilm Wako Pure Chemical). The residual photoresist on FTO patterns was removed by dipping in acetone (Guaranteed Reagent, Fujifilm Wako Pure Chemical).
2. TiO_2 photoanode deposition: Next, mesoporous TiO_2 was formed by the calcination of PEG containing a sol–gel precursor. As reported in the literature, the surface area of mesoporous TiO_2 can be varied by changing the molecular weight of the added PEG.[12,21,22] The patterned TiO_2 photoanode was formed by spin-coating on the masked FTO layer. The TiO_2 sol–gel precursor was prepared by adding 10 mL of deionized water and 1 mol% PEG into a mixture solution of 1.25 mL of titanium isopropoxide (TTIP) (95%, Fujifilm Wako Pure Chemical), 10 mL of ethanol (99.5%, Fujifilm Wako Pure Chemical), and 0.3 mL of HCl. The TiO_2 sol–gel precursor on the substrate was dried at 100 ºC for 10 min, and the substrate temperature was increased for annealing at 500 ºC for 1 h.
3. Pt cathode and co-catalyst deposition: The Pt cathode and co-catalyst patterns were deposited by sputtering with a stencil mask after the deposition of the Ti adhesive layer. Stencil masks were prepared by forming holes on 60-mm-thick Ni foils by wet etching with 1.2 mol/L $FeCl_3$ aqueous solution.

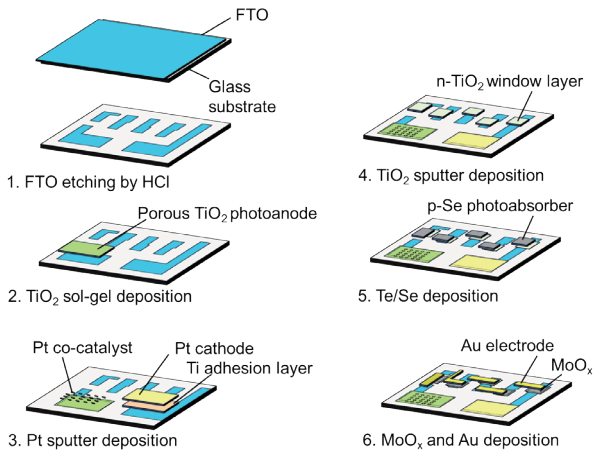

Fig. 2. (Color online) Fabrication of the proposed water-splitting device composed of TiO_2-based PEC and serially connected Se thin PV devices on a chip.

4. n-type TiO_2 window layer deposition: The TiO_2 window layer (50 nm) was deposited by reactive sputtering with a Ti metal target (4 N, Ti, 50.8 mm in diameter, 5 mm in thickness, Furuuchi Chemical Co.).[16,17,23] The sputtering chamber was evacuated using a turbo molecular pump to a base pressure below 1×10^{-3} Pa. Argon gas was introduced at the desired partial pressure (P_{Ar}) of 0.1 Pa. Oxygen gas was also introduced at a partial pressure (P_{O_2}) of 0.3 Pa. The total pressure was set as 6 Pa at the substrate temperature of 350 °C. The film deposition was conducted with an RF power at 300 W. TiO_2 thin films were patterned by sputtering through a stencil mask.
5. Te/Se deposition: A very thin Te layer was inserted between the Se and TiO_2 layers to improve the adhesion between these layers. Te and Se layers were sequentially deposited by thermal evaporation. After Se deposition, Se/Te stacked layers were annealed at 200 °C for 2 min to crystallize the Se/Te layers.[10,23–25] The Te thickness was controlled by evaporating all the weighed Te debris because it is difficult to form 1-nm-thick films using a thickness monitoring system. Se/Te layers were patterned by evaporation through a stencil mask.
6. MoO_x and Au deposition: The MoO_x (20 nm) and Au (150 nm) hole injection layers were deposited by thermal evaporation through stencil masks.

3. Results and Discussion

3.1 Preliminary characterization of water splitting

In a preliminary experiment, PEC and PV performance characteristics were characterized using the separated devices to simplify the characterization procedure, considering the yield rate of manufacturing devices. Bias voltages supplied to PEC were varied using both a wired external electrical power source and the separated PV devices in the first step of characterization.

PEC devices without PV devices were prepared by fabrication steps 1–3 described in Sect. 3. A photograph of the fabricated PEC and SEM and AFM images of the mesoporous TiO_2 photoanode are shown in Figs. 3(a)–3(c), respectively. The surface roughness and morphology of the TiO_2 thin films were evaluated by scanning at a rate of 1.0 Hz using a dynamic atomic force microscope (DFM, MFP-3D-BIO, Asylum Research Corp., CA, USA). A rough morphology of porous TiO_2 can be observed in Fig. 3(c). The root mean square surface roughness (R_{RMS}) of the mesoporous TiO_2 photoanode was measured to be 262 nm. The effects of increasing the surface area of TiO_2 at R_{RMS} larger than 262 nm on enhancing photocatalytic activity have been reported.[23,26] For example, Latthe *et al.* previously reported that the photocurrent density in cyclic voltammetry with light illumination was increased seven times by increasing the surface roughness of the supersonic aerosol-coated TiO_2 thin films from R_a = 350 to 710 nm.[27] Thus, further optimization of the surface morphology is considered to be effective for enhancing the photocatalytic reaction. An open circuit voltage of approximately 3.2 V can be supplied to the TiO_2 photocatalyst by the five serially connected PV cells to support the water-splitting reaction. The PEC shown in Fig. 3(a) is composed of a Pt cathode and a TiO_2 photoanode for hydrogen and oxygen generation, respectively.

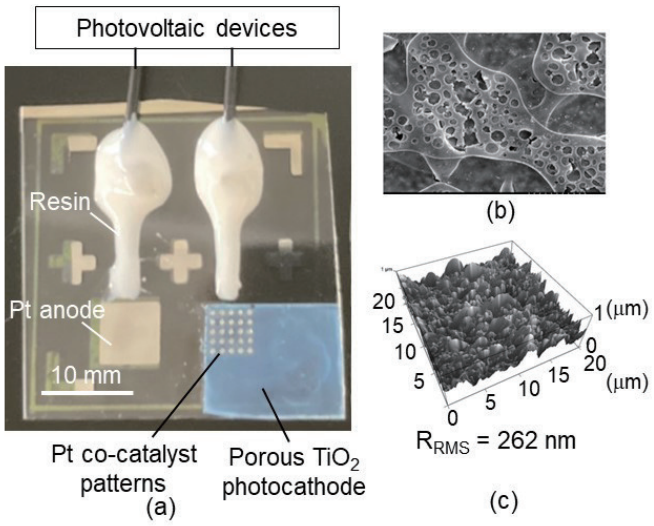

Fig. 3. (Color online) (a) Photograph of the fabricated PEC and (b) SEM and (c) AFM images of mesoporous TiO_2 photoanode.

The water-splitting reaction was characterized using the fabricated PEC with an acrylic attachment. Ambient pressure, the type of chemical additive in the aqueous solution, and bias voltage applied to the TiO_2 photoanode are known to be effective parameters in the water-splitting reaction. These parameters were varied, and the generated volume of hydrogen was measured. An acrylic attachment with gas reservoirs was designed to observe the water-splitting reaction and measure gas volume as parameters such as pressure, bias voltages and area percentage of co-catalyst on TiO_2 photoelectrode and their combination are varied. The generated gas volume was estimated by measuring the reserved gas volume, as shown in Fig. 4(a). Ambient pressure can be adjusted by evacuation to the targeted pressure while monitoring the pressure gauge. Bias voltages can be applied to the photoanode through the flange with hermetic seal under negative pressure conditions. The acrylic chamber was filled with an electrolyte solution in such a way that the pressure-measuring port is not completely immersed. The water-splitting reaction was started by UV illumination from the back of the substrate and supplying bias voltage. The UV-LED (peak wavelength at 365 nm, FOLS-09) was used at an intensity of 10 mW/cm^2 in this experiment. Figure 4(b) shows a photograph of the fabricated reactor chamber. Gas volumes that accumulated in reservoirs as a function of time were measured.

PV devices without PEC were prepared by fabrication steps 4–6 described in Sect. 3. A photograph of the simplified PV device is shown in Fig. 5.

The active area of a single TiO_2/Se PV device shown in Fig. 5 was designed to be 4 mm^2. The measurement results of current density and voltage curves for (a) a single PV device and (b) a serially connected PV device (five cells) with and without light illumination are shown in Fig. 6. Light illumination was conducted at 100 mW/cm^2 at AM 1.5 using a solar simulator (OTENTO-SUNIII, Bunkoukeiki Co., Ltd., Japan). It was observed in Figs. 6(a) and 6(b) that the open

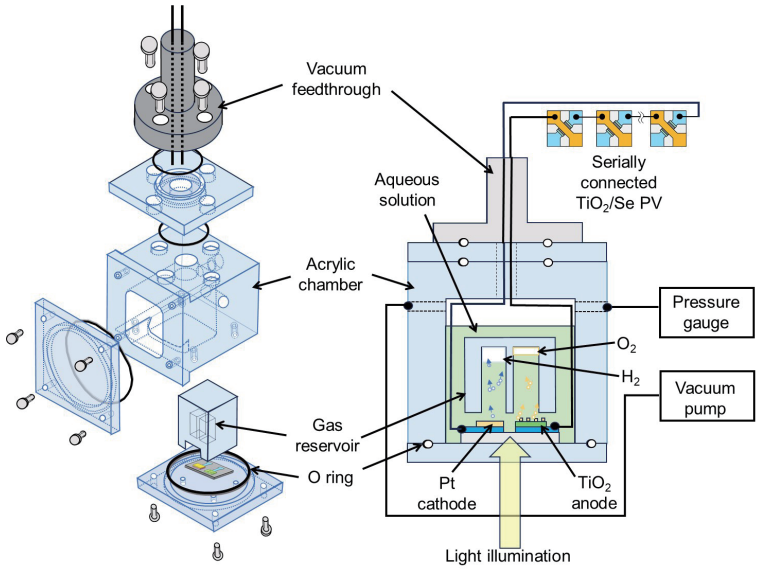

(a)

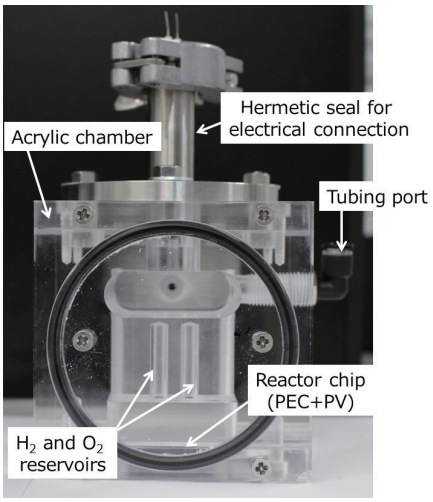

(b)

Fig. 4. (Color online) (a) Structure of acrylic attachment with gas reservoirs for the observation of water-splitting reaction and measurement of gas volumes as parameters such as pressure, bias voltages and area percentage of co-catalyst on TiO_2 photoelectrode and their combination are varied. (b) Photograph of the fabricated acrylic reaction chamber.

circuit voltage was increased from 0.69 to 3.32 V by connecting five PV cells serially. The serially connected device had lower short-circuit current density and fill factor than the single PV device. This is probably a result of the increased resistance at the connecting parts between the five cells and/or the inadequate matching of the photocurrent from individual PV cells. This is also caused by the inadequate performance homogeneity of plural photovoltaic cells on a substrate by our laboratory equipment. It will be important to improve the uniformity of PV performance to decrease the mismatched current of serially connected PV cells. Decreasing the

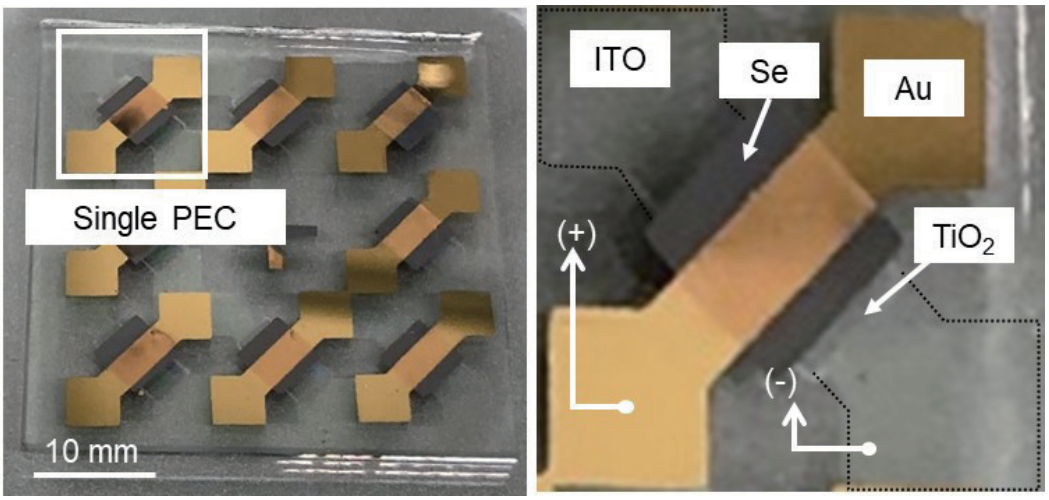

Fig. 5. (Color online) Photograph of the fabricated PV device and magnified photograph of a single PEC device.

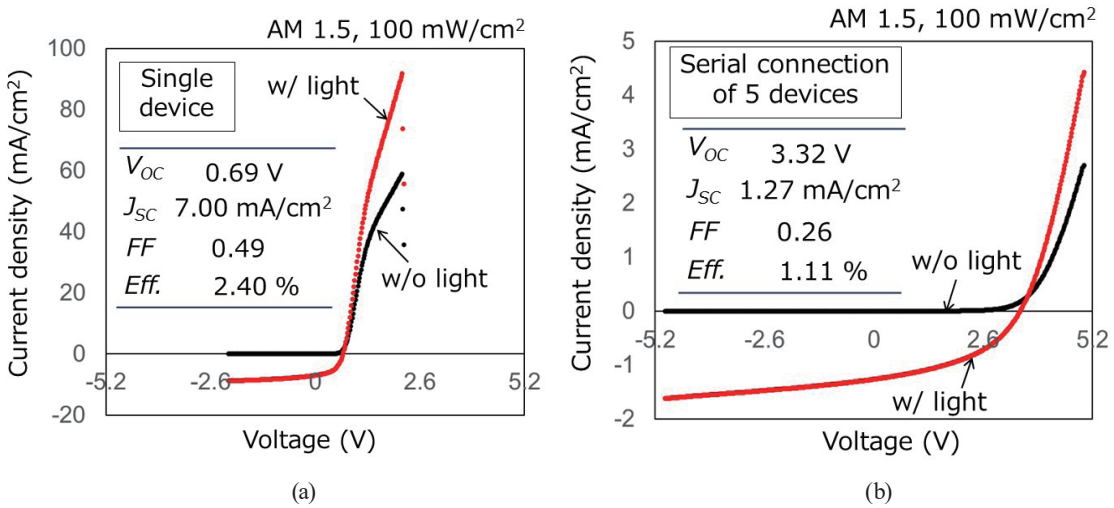

Fig. 6. (Color online) Measurement results of current density and voltage curves for (a) a single PV device and (b) a serially connected PV device (five cells) with and without light illumination at 100 mW/cm^2 at AM 1.5.

distance between individual photovoltaic cells is also suggested as an effective approach to decreasing the electrical resistance at connecting parts.

A photograph of the fabricated PEC with the wire-connected PV devices used for the preliminary characterization of water splitting and its demonstration are shown in Figs. 7(a) and 7(b), respectively. It can be observed in Fig. 7(b) that the generated oxygen was accumulated in the reservoir. However, it was difficult to measure the hydrogen volume accurately because hydrogen bubbles adhered strongly to the Pt electrode. Thus, the hydrogen volume was calculated to be two times the oxygen volume.

The generated hydrogen volumes as a function of UV illumination time with and without Pt co-catalyst patterns on the TiO_2 photoanode are shown in Fig. 8, when a bias voltage of 3.2 V

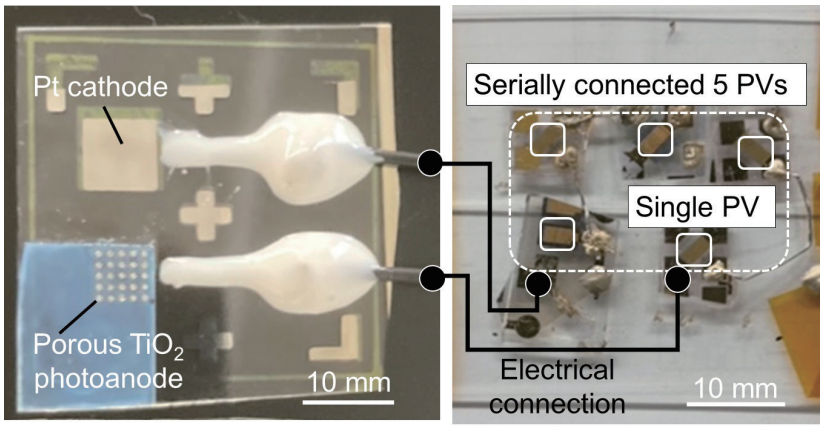

(a)

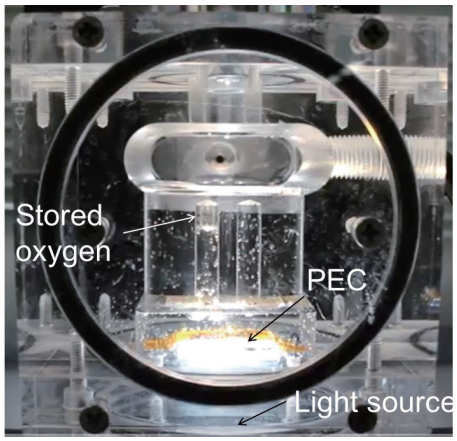

(b)

Fig. 7. (Color online) Photographs of (a) PEC with the wire-connected PV devices for preliminary water-splitting characterization and (b) water-splitting demonstration.

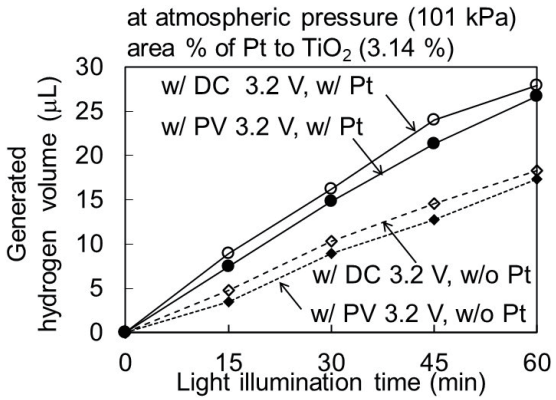

Fig. 8. Generated hydrogen volume as a function of UV illumination time, when the experiment was conducted at the ambient pressure of 101 kPa. A bias voltage of 3.2 V was supplied by the wire-connected DC electrical power source and the wire-connected serially connected PV devices.

was supplied by the wire-connected DC electrical power source and the wire-connected serially connected TiO_2/Se PV devices. The areal percentage of Pt to TiO_2 was fixed at 3.14%. Five PV devices were serially connected, and the open circuit voltage of the connected PV was 3.2 V with one-sun illumination. UV was also applied to the sol–gel-derived TiO_2 photoanode. It was observed in Fig. 8 that the rate of hydrogen generation increased from 18.3 to 27.9 μL/h upon adding the Pt co-catalyst to the TiO_2 photoanode when a bias voltage of 3.2 V was supplied by the DC power source. It was also observed in Fig. 8 that the rate of hydrogen generation increased from 17.4 to 26.7 μL/h upon adding the Pt co-catalyst to the TiO_2 photoanode when a bias voltage of 3.2 V was supplied by the serially connected TiO_2/Se PV devices. These results indicate that the photocatalytic reaction is enhanced by suppressing the hole-electron recombination due to the creation of an electrical potential gradient at the Pt/TiO_2 Schottky interface.[1,14] The TiO_2-Pt PEC with bias voltages supplied by DC and PV power sources exhibited water-splitting performance similar that of the TiO_2 electrode.

The generated hydrogen volume as a function of time is shown in Fig. 9, when the pressure in the acrylic chamber was varied. Generally, photocatalytic water splitting reactivity decreases with increasing ambient pressure because of the activation of back reactions such as water formation by hydrogen and oxygen molecules and/or the photoreduction of those molecules.[28,29] At high pressures, the photocatalytic activity for overall water splitting generally decreases because of the slower bubble formation and desorption of product gases.[28] An open circuit voltage of 3.2 V was applied to the PEC from the wire-connected TiO_2/Se PV devices by the same procedure as described in the explanation for Fig. 8. It was seen that the rate of hydrogen generation increased with decreasing pressure. The volume of hydrogen generated at a pressure of 20 kPa reached almost five times that obtained in air atmosphere.

The saturation tendencies of hydrogen production were observed at lower pressures as shown in Fig. 9. One of the possible reasons for that may be the increased back reaction due to the increased oxygen and hydrogen amounts with decreasing ambient pressure. The reactive surface

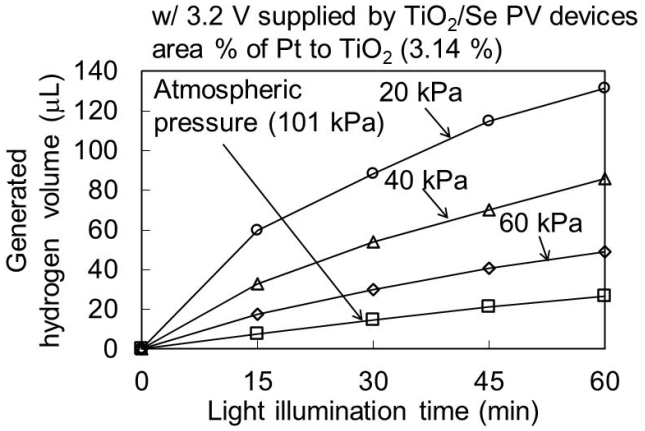

Fig. 9. Generated hydrogen volume as a function of UV light illumination time, when the pressure in the acrylic chamber was varied. An open circuit voltage of 3.2 V was applied to the PEC from the wire-connected TiO_2/Se PV devices by the same procedure as described in the explanation of Fig 8.

area of the Pt cathode was considered to be smaller than that of the porous TiO_2 photoanode. Thus, the reaction rate limitation at the Pt cathode is also considered as the other possible reason for the nonlinear tendency of hydrogen production when ambient pressure was decreased. The optimization of device dimensions is one of our future works. The effects of adding a Pt co-catalyst with TiO_2 on the water-splitting activity were characterized at a constant pressure of 20 kPa. A co-catalyst such as Pt or Au is considered to suppress the back reaction of molecules in photocatalytic water splitting.[13] According to the literature, the excessively large percentages of the Pt co-catalyst to the TiO_2 photocatalyst cause reaction limitation because of the trade-off between the decreased photon absorption due to a Pt shadow and the promotion of the reaction.[30] The number of pieces of Pt co-catalyst circle shaped patterns (200 um in diameter) was varied as 0, 5, 10, 15, 20, and 25. The Pt co-catalyst patterns were formed as circular dots of 200 mm diameter. The area ratios of Pt to TiO_2 were 0.63, 1.26, 1.89, 2.51, and 3.14%. The calculated hydrogen volume as a function of time is shown in Fig. 10. It is suggested that the generated hydrogen volume increased with the area ratio of Pt to TiO_2. TiO_2 supported with Pt at an area ratio of 3.14 % increased the amount of hydrogen generated to 1.5 times larger than that without a co-catalyst. On the other hand, the rate of increase in the amount of hydrogen generated showed a saturation tendency with increasing Pt area. This may be a result of the reverse reaction from gas to water at the Pt surface with increasing Pt area. In addition, the excessively increased hydrogen production may cause the increased back reaction.

The hydrogen production reactor for a mobile power source is one of our future applications. In this study, the hydrogen production rate can be calculated as 5.36 mmol/h using a TiO_2 photoanode with a 17 × 14 mm^2 projection area. Further increasing the hydrogen production rate up to sub-mol/h will become one of our future works. As a reference, it has been reported that a methanol fuel processor with dimensions of 70 × 40 × 30 mm^3 demonstrated hydrogen production at 0.498 mol/h for the estimated electric power of 15 W.[31] From the viewpoint of application for hydrogen fuel cells, 15 µL per W/min was reported as an example of the hydrogen consumption rate.[32] Therefore, it will be necessary to increase the hydrogen production rate by approximately twofold.

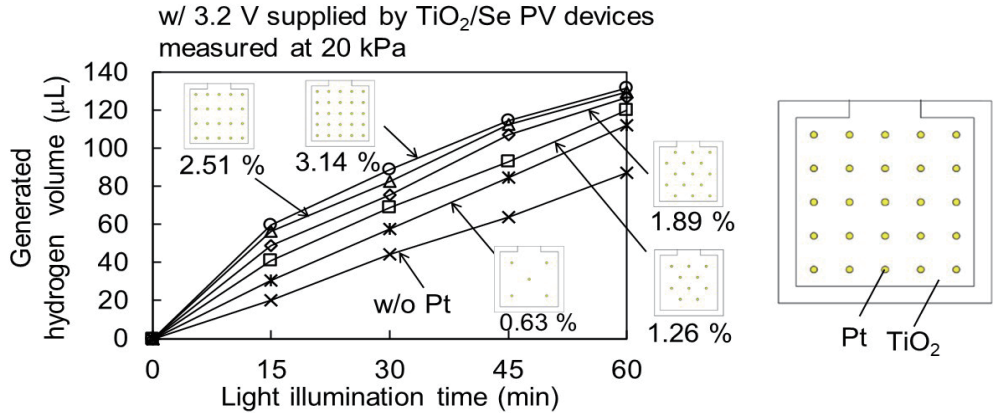

Fig. 10. (Color online) Generated hydrogen volume as a function of time, when the area ratio of Pt co-catalyst to TiO_2 photoanode was varied. The number of pieces of Pt co-catalyst circle shaped patterns (200 um in diameter) was varied as 0, 5, 10, 15, 20, and 25. The area ratios of Pt to TiO_2 were 0.63, 1.26, 1.89, 2.51, and 3.14% at a constant pressure of 20 kPa.

3.2 Water-splitting demonstration using device with TiO_2/Se PV integrated with TiO_2-Pt PEC devices

The TiO_2/Se PV device and TiO_2-based PEC were integrated and connected to each other on a 30 × 30 mm^2 chip, as shown in Fig. 11. Five PV devices were serially connected, and the open circuit voltage of the connected PV was 3.2 V with one-sun illumination. UV was also applied to the sol–gel-derived TiO_2 photoanode under the same conditions as in the preliminary experiment. The hydrogen volume as a function of light illumination time is shown in Fig. 12, when a bias voltage of 3.2 V was supplied from an external voltage source and the serially connected PV devices on a chip. The hydrogen generation rate was calculated from the reserved oxygen volume to be 26.6 μL/h. The PEC and PV integrated device on a chip showed a smaller volume of hydrogen generated. The increased series resistance due to the serial connection of PV devices is considered to be one of the possible reasons for the smaller hydrogen volume.

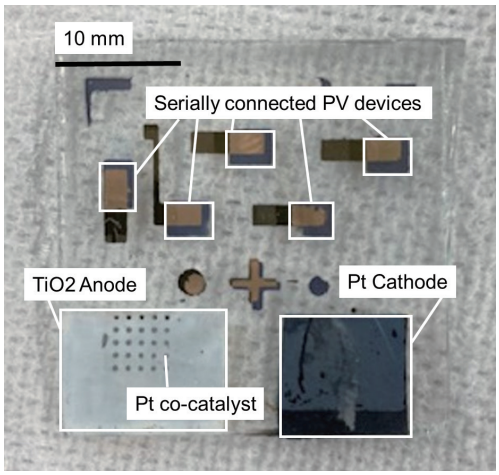

Fig. 11. (Color online) Photograph of TiO_2/Se PV devices and TiO_2-based PEC integrated and connected to each other on a 30 × 30 mm^2 chip.

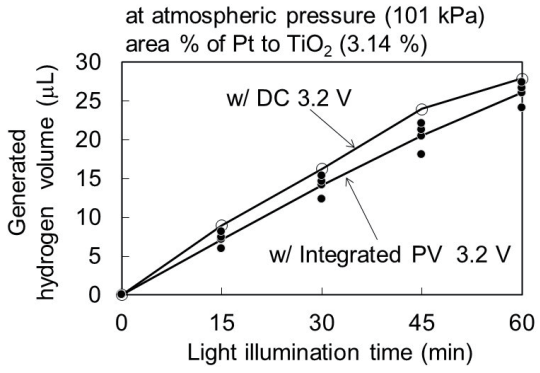

Fig. 12. Hydrogen volume as a function of light illumination time, when a bias voltage of 3.2 V was supplied from an external voltage source and serially connected PV devices on a chip.

4. Conclusions

Compact fuel cells such as PEFC have recently attracted considerable attention in terms of applicable power supply for indoor small appliances such as IoT devices. Thus, it is considered that a miniaturized hydrogen generator will become more important for such applications. Microreactor technology enables a reduction of risk in terms of the use of reactive and/or toxic materials, and its compactness will be suitable for mobile on-site hydrogen generation applications. In this work, a water-splitting device composed of a combination of a TiO_2 photocatalyst and a PV bias voltage source on a chip was developed. The water-splitting reaction was successfully induced by only light illumination without the need for an external wired electrical power source.

Acknowledgments

The authors would like to acknowledge the support of the Mazda Foundation.

References

1 A. Körner: Technology Roadmap. Hydrogen and Fuel Cells (OECD/IEA, Paris, 2015). https://doi.org/10.1787/9789264239760-en
2 B. A. Pinaud, J. D. Benck, L. C. Seitz, A. J. Forman, Z. Chen, T. G. Deutsch, B. D. James, K. N. Baum, G. N. Baum, S. Ardo, H. Wang, E. Miller, and T. F. Jaramillo: Energy Environ. Sci. **6** (2013) 1983. https://doi.org/10.1039/c3ee40831k
3 J. Brillet, M. Cornuz, F. L. Formal, J.-H. Yum, M. Grätzel, and K. Sivula: J. Mater. Res. **25** (2010) 17. https://doi.org/10.1557/JMR.2010.0009
4 T. J. Jacobsson, V. Fjällström, M. Edoff, and T. Edvinsson: Energy Env. Sci. **7** (2014) 2056. https://doi.org/10.1039/C4EE00754A
5 J. Jia, L. C. Seitz, J. D. Benck, Y. Huo, Y. Chen, J. W. D. Ng, T. Bilir, J. S. Harris, and T. F. Jaramillo: Nat. Commun. **7** (2016) 13237. https://doi.org/10.1038/ncomms13237
6 Z. Wang, C. Li, and K. Domen: Chem. Soc. Rev. **48** (2019) 2109. https://doi.org/10.1039/C8CS00542G
7 X. Pan, X. Hong, L. Xu, Y. Li, M. Yan, and L. Mai: Nano Today **28** (2019) 100764. https://doi.org/10.1016/j.nantod.2019.100764
8 C. Liu, J. Tang, H. M. Chen, B. Liu, and P. Yang: Nano Lett. **13** (2013) 2989. http://doi.org/10.1021/nl1401615t
9 O. Khaselev and J. A. Turner: Science **280** (1998) 425. https://doi.org/10.1126/science.280.5362.425
10 T. Kobayashi and S. Konishi: 2017 19th Int. Conf. Solid-State Sensors, Actuators and Microsystems (TRANSDUCERS) (2017) 359. https://doi.org/10.1109/TRANSDUCERS.2017.7994062
11 K. Shimakura, S. Saeki, Y. Segawa, and T. Kobayashi: IEEJ Trans. Sensor and Micromachines **142** (2022) 182. https://doi.org/10.1002/ecj.12381
12 T. Balaganapathi, B. Kaniamuthan, S. Vinoth, and P. Thilakan: Mater. Chem. Phys. **189** (2017) 50. https://doi.org/10.1016/j.matchemphys.2016.12.016
13 S. S. Arbuj, R. R. Hawaldar, U. P. Mulik, B. N. Wani, D. P. Amalnerkar, and S. B. Waghmode: Mater. Sci. Eng., B **168** (2010) 90. https://doi.org/10.1016/j.mseb.2009.11.010
14 S. Ito, K. Shimakura, Y. Tanaka, D. Yamane, and T. Kobayashi: IEEJ Trans. Sensors and Micromachines **143** (2023) 231. https://doi.org/10.1541/ieejsmas.143.231
15 T. Kobayashi, H. Maeda, and S. Konishi: Jpn. J. Appl. Phys. **55** (2016) 06GP03. https://doi.org/10.7567/JJAP.55.06GP03
16 T. Kobayashi and S. Konishi: J. Micromech. Microeng. **25** (2015) 115014. https://doi.org/10.1088/0960-1317/25/11/115014
17 T. Kobayashi and S. Konishi: Surf. Coat. Technol. **363** (2019) 80. https://doi.org/10.1016/j.surfcoat.2019.02.043
18 R. Abe, K. Sayama, and H. Arakawa: Chem. Phys. Lett. **371** (2003) 360. https://doi.org/10.1016/S0009-2614(03)00252-5

19 N. Rozman, P. Nadrah, R. Cornut, B. Jousselme, M. Bele, G. Dražić, M. Gaberšček, Š. Kunej, and A. S. Škapin: Int. J. Hydrogen. Energy **46** (2021) 32871. https://doi.org/10.1016/j.ijhydene.2021.07.129
20 B. Yan, X. Liu, W. Lu, M. Feng, H.-J. Yan, Z. Li, S. Liu, C. Wang, J.-S. Hu, and D.-J. Xue: Sci. Adv. **8** (2022) eadc9923. https://doi.org/10.1126/sciadv.adc9923
21 S. Bu, Z. Jin, X. Liu, L. Yang, and Z. Cheng: Mater. Chem. Phys. **88** (2004) 273. https://doi.org/10.1016/j.matchemphys.2004.03.033
22 J. M. Calderon-Moreno, S. Preda, L. Predoana, M. Zaharescu, M. Anastasescu, M. Nicolescu, M. Stoica, H. Stroescu, M. Gartner, O. Buiu, M. Mihaila, and B. Serban: Ceram. Int. **40** (2014) 2209. https://doi.org/10.1016/j.ceramint.2013.07.139
23 T. Kawagishi, Y. Adachi, and T. Kobayashi: Mater. Chem. Phys. **297** (2023) 127371. https://doi.org/10.1016/j.matchemphys.2023.127371
24 J. Fujimura, Y. Adachi, T. Takahashi, and T. Kobayashi: Nano Energy **99** (2022) 107385. https://doi.org/10.1016/j.nanoen.2022.107385
25 T. K. Todorov, S. Singh, D. M. Bishop, O. Gunawan, Y. S. Lee, T. S. Gershon, K. W. Brew, P. D. Antunez, and R. Haight: Nat. Commun. **8** (2017) 682. http://doi.org/10.1038/s41467-017-00582-9
26 M. Ibadurrohman and K. Hellgardt: ACS Appl. Mater. Interfaces **7** (2015) 9088. https://doi.org/10.1021/acsami.5b00853
27 S. S. Latthe, S. An, S. Jin, and S. S. Yoon: J. Mater. Chem. A **1** (2013) 13567. https://doi.org/10.1039/c3ta13481d
28 Q. Wang, T. Hisatomi, Y. Suzuki, Z. Pan, J. Seo, M. Katayama, T. Minegishi, H. Nishiyama, T. Takata, K. Seki, A. Kudo, T. Yamada, and K. Domen: J. Am. Chem. Soc. **139** (2017) 1675. https://doi.org/10.1021/jacs.6b12164
29 T. Hisatomi, J. Kubota, and K. Domen: Chem. Soc. Rev. **43** (2014) 7520. https://doi.org/10.1039/C3CS60378D
30 B. You and Y. Sun: Acc. Chem. Res. **51** (2018) 1571. https://doi.org/10.1021/acs.accounts.8b00002
31 J. D. Holladay, Y. Wang, and E. Jones: Chem. Rev. **104** (2004) 4767. https://doi.org/10.1021/cr020721b
32 R. Rath, P. Kumar, S. Mohanty, and S. K. Nayak: Int. J. Energy Res. **43** (2019) 8931. https://doi.org/10.1002/er.4795

About the Authors

Kenichi Takatsuki received his B.S. degree from Ritsumeikan University, Shiga, Japan, in 2023. Since 2023, he has been a master course student at Ritsumeikan University.

Riku Takahashi received his B.S. degree in 2021 and M.S. degree in 2023 in mechanical engineering from Ritsumeikan University, Shiga, Japan. He is currently working at Mitsubishi Electric Inc.

Taizo Kobayashi received his B.S. degree in 1999, M.S. degree in 2001, and Ph.D. degree in 2009 in mechanical engineering from Ritsumeikan University, Shiga, Japan. His research focuses on optical functional materials in MEMS applications. He is currently a professor at Ritsumeikan University, where he joined the faculty in 2017. (tkt07004@fc.ritsumei.ac.jp)